Available online at www.sciencedirect.com
SCIENCE DIRECT®
Catalysis Today 96 (2004) 43–52
CATALYSIS TODAY
www.elsevier.com/locate/cattod

Study of the effect of Ba loading for catalytic activity of Pt–Ba/Al_2O_3 model catalysts

L. Castoldi, I. Nova*, L. Lietti, P. Forzatti

Dipartimento di Chimica, Materiali e Ingegneria Chimica "Giulio Natta", Politecnico di Milano, Piazza Leonardo da Vinci 32, 20133 Milan, Italy

Available online 25 June 2004

Abstract

A series of Pt–Ba/Al_2O_3 NO_x storage-reduction (NSR) catalysts having different Ba loadings (in the range 0–30%, w/w) have been prepared, characterized and tested in the NO_x adsorption-reduction under realistic operating conditions. Accordingly, the role of the Ba loading on the storage of NO_x and on their subsequent reduction has been addressed.

The results indicated that the presence of Ba negatively affects both the catalyst morphological properties and the Pt dispersion in the samples with Ba loading higher than 10%, while a strong increase of the NO_x adsorption capacity is observed. This effect has been associated to the involvement in the NO_x storage process of Pt–Ba neighboring species. The analysis of the storage phase also showed that the highest the Ba content, the lowest the NO_2 concentration at catalyst saturation: this effect has been related to the decrease in the Pt content of the catalyst following Ba addition to the samples and/or to a possible masking of Pt sites when the Ba coverage approaches and exceeds the monolayer capacity of the support.

Concerning the reduction phase, the data pointed out that for all the investigated catalysts the stored NO_x species are readily reduced upon H_2 admission: nevertheless, the reduction process resulted very complex and it can lead to nitrogen and/or ammonia depending on the formulation and properties of the catalysts.

Keywords: Lean NO_x traps; NSR catalysis; Pt–Ba/Al_2O_3 catalyst; Ba loading; NO_x storage and reduction

1. Introduction

The demand to improve the fuel efficiency of vehicles and the need to decrease the CO_2 emissions has recently led to the introduction of the so-called lean-burn engine technology, where the engine is operated in the presence of excess oxygen. This type of engine operation can effectively reduce the fuel consumption and provide a more efficient combustion in comparison with stoichiometric operating conditions [1]. However, the presence of excess oxygen under lean-burn conditions strongly decreases the efficiency of the catalytic reduction of NO_x of the three-way catalyst, which are normally used after engines operated under stoichiometric conditions. Accordingly, a variety of strategies are currently being investigated to solve the problem.

A possible solution involves the use of a NO_x storage-reduction (NSR) catalyst in combination with mixed-lean engine operation, as developed and introduced by Toyota during the mid-1990s [1]. The NSR catalyst consists of a storage component based on an alkaline earth metal oxide (e.g. BaO) and a precious metal, generally Pt, dispersed on γ-Al_2O_3. One typical example of this class of catalysts is the Pt–Ba/γ-Al_2O_3 system [1,2]. The basic concept of the NSR catalyst is a cyclic process during which the storage of NO_x is accomplished under lean conditions and the subsequent catalyst regeneration is carried out during a short period under rich conditions.

The catalytic behavior of Pt–Ba model system in the reduction of NO_x under NSR conditions is object of several papers in the literature.

In particular, the NO_x storage process has been extensively investigated by dynamic methods [3–7] and in situ spectroscopy [8–13] and the kinetic modeling as well [14–18]; different mechanisms have been proposed for the adsorption of NO_x. It is commonly believed that NO_2 is

* Corresponding author. Tel.: +39-02-2399-3228; fax: +39-02-7063-8173.
E-mail address: isabella.nova@polimi.it (I. Nova).

0920-5861/$ – see front matter © 2004 Elsevier B.V. All rights reserved.
doi:10.1016/j.cattod.2004.05.006

responsible for the NO_x adsorption process [2,5,13]; in this respect, since the exhausts contain NO/O_2, the first step of the storage process is thought to be the oxidation of NO to NO_2, followed by the adsorption of NO_2 on barium in the form of nitrates.

In our recent works [11,17,19], we have presented a different picture on the adsorption process over Pt–Ba/γ-Al_2O_3 catalyst starting from NO/O_2 mixture. Comparing data from pulse experiment and FT-IR spectra recorded upon NO/O_2 addition, we have proposed that the storage process is accomplished via two parallel routes, which imply: (i) a stepwise oxidation of NO in the presence of oxygen to form nitrite ad-species, which are progressively oxidized to nitrates ("nitrite route") and (ii) the oxidation of NO to NO_2, and its subsequent adsorption via disproportionation to form nitrates ("nitrate route"). It has also been suggested that the presence of Pt–Ba couples (i.e. the existence of a Pt–Ba interaction) might be relevant for the "nitrite" route. In this respect, it is of interest to investigate the effect of the catalyst Ba loading, since it is expected that this would affect the Pt–Ba interaction and hence the catalyst performances. As a matter of fact, the analysis of recent literature showed that a relatively limited number of investigations have been performed in order to analyze the effect of the barium content on the catalytic activity of Pt loaded γ-alumina catalysts. Fanson et al. [20] compared on the basis of FT-IR data the storage capacity of Pt–Ba/γ-Al_2O_3 systems with 8 and 26% (w/w) of barium at 450 °C with NO/O_2 mixtures and conclude that only the catalyst with the highest Ba loading is able to adsorb significant amounts of NO_x. Mahzoul et al. [3] studied the NO_x adsorption over commercial NSR catalysts supplied by Johnson Matthey in powder form, with different Ba loading. The experimental results showed that the higher the Ba content of the samples, the higher the storage capability of the systems. This datum was confirmed by Laurent et al. [18] who studied the effect of BaO content (in the range 10–20%, w/w) on a Pt(1)–Ba/alumina commercial catalyst. In particular, by analyzing the adsorption of NO/O_2 mixtures at 300 °C, these authors found that the storage capacity of the systems increased proportionally to the catalyst Ba content. Finally, Hess and Lunsford [21] investigated the mechanism of NO_2 storage on barium oxide supported on magnesium oxide. In their work, the coverage-dependent storage behavior was also investigated by comparing 7 mol% BaO/MgO and 14 mol% BaO/MgO. On the basis of Raman spectroscopy results the authors showed that the NO_2 storage capacity of BaO/MgO increases with Ba loading.

In order to better analyze these aspects, in this work a series of Pt–Ba/Al_2O_3 NSR catalysts containing different Ba loadings (in the range 0–30%, w/w) have been prepared, characterized and tested in the NO_x adsorption–reduction under realistic operating conditions. Accordingly, the role of the Ba loading on the storage of NO_x and on their subsequent reduction could be analyzed.

2. Experimental

2.1. Material preparation and characterization

The catalysts were Pt highly dispersed over a γ-Al_2O_3 carrier, loaded with various amounts of Ba. The preparation procedure involved two sequential impregnation steps as follows. A powder γ-Al_2O_3 carrier (Versal 250 from La Roche Chemicals, surface area of 200 m^2/g and pore volume of 1.4 cm^3/g) was at first impregnated with a solution of $Pt(NH_3)_2(NO_2)_2$ (Strem Chemicals, 5% Pt in ammonium hydroxide) with an appropriate concentration so as to yield 1 wt.% Pt metal loading. After drying in air for 12 h at 80 °C and calcination at 500 °C for 5 h, batches of this sample were impregnated with solutions containing various concentrations of $Ba(CH_3COO)_2$ (Strem Chemical, 98.5%). The solution concentrations were appropriately chosen so as to yield samples with Ba loadings in the range 0–30 wt.%. The impregnated samples were initially dried for 12 h at 80 °C and then calcined at 500 °C for 5 h. The powder materials prepared in this work are listed in Table 1 in term of percent w/w for each component.

Surface area and pore size distribution were determined by N_2 adsorption–desorption at 77 K with the BET method using a Micromeritics TriStar 3000 Instrument.

The Pt dispersion was estimated from hydrogen chemisorption at 0 °C after reduction in H_2 at 300 °C using a TPD/R/O 1100 ThermoElectron Corporation Instrument.

XRD spectra were collected on powder samples calcined at 500 °C with a Brüker D8 Advanced Instrument equipped with graphite monochromator on the diffracted beam.

2.2. Catalytic tests

The adsorption of NO_x under transient conditions has been investigated by the transient response method (TRM) by using a flow micro-reactor system made of a quartz tube (7 mm ID) inserted into an electric furnace driven by a PID temperature controller/programmer. The temperature of the catalyst was measured and controlled by a K-type thermocouple (o.d. = 0.5 mm) directly immersed in the catalyst bed. The flow rate of the

Table 1
Composition (wt.%) of Pt, Ba and Al_2O_3 in the catalysts used in this study

Sample name	Composition (wt.%)		
	γ-Al_2O_3	Pt	Ba
Pt–Ba(0)	99.0	0.99	0
Pt–Ba(5)	94.1	0.95	4.95
Pt–Ba(10)	89.1	0.90	10
Pt–Ba(16)	82.6	0.83	16.5
Pt–Ba(23)	76.4	0.77	22.78
Pt–Ba(30)	69.5	0.70	29.79

feed gases was measured and controlled by mass-flow controllers (Brooks 5850 TR), and the gases were mixed in a single stream before entering the reactor. Two four-port valves were used to perform the abrupt switches in the inlet gas-phase composition. The reactor outlet was directly connected to a mass spectrometer (Balzers QMS 200); care was taken to minimize all possible dead volumes in the lines before and after the reactor and in eliminating pressure and flow changes upon switching of the feed gases. The following mass-to-charge (*m*/*e*) ratios were used to monitor the concentration of products and reactants: 18 (H_2O), 28 (N_2 or CO), 30 (NO), 32 (O_2), 44 (N_2O or CO_2), and 46 (NO_2). The mass spectrometer data were quantitatively analyzed using the fragmentation patterns and the response factors determined experimentally from calibration gases. A gas chromatograph (HP 6890) equipped with a Poraplot Q and a 5 Å molecular sieve capillary column was also used for the analysis of CO_2, N_2O and H_2O, and of O_2, N_2 and CO, respectively.

In a typical experiment, 120 mg of catalyst sample was loaded in the reactor and treated at 500 °C in He + 3% O_2 (3.33 cm^3/s at Standard Temperature Pressure, STP); then the catalyst temperature was set at 350 °C. After stabilization of the mass spectrometer signals, a rectangular step feed of NO (1000 ppm) was admitted at constant temperature. The NO_x storage was allowed to proceed up to catalyst saturation; then the inlet NO concentration was decreased stepwise to zero. The subsequent catalyst reduction procedure (i.e., the removal of the stored NO_x) was accomplished by imposing a stepwise addition of H_2 to the reactor (0 → 2000 ppm and 2000 → 0 ppm in He).

3. Results and discussion

3.1. Catalyst characterization

The results of the morphological characterization carried out over all the prepared samples are reported in Fig. 1 in terms of surface area (A_s), pore volume (V_p) and Pt dispersion. The Pt–Ba(0) sample is characterized by large surface area (186 m^2/g) and pore volume (1.02 cm^3/g). When the binary sample is impregnated with a barium solution, the resulting catalysts show a decrease in the surface area and in the pore volume. The pore radius (not shown in the figure) is always in the range 90–110 Å.

The Pt dispersion, measured by H_2 chemisorption at 0 °C, is about 82% in Pt–Ba(0) and decreases upon addition of Ba reaching the value of 40% at the highest barium loading. The decrease in the Pt dispersion is likely due to the fast and exothermic decomposition of Barium acetate precursor, eventually leading to sintering of the Pt crystallites, and/or to the masking of the Pt crystallites by the Ba component. Accordingly, the thermal analysis DTA-TG (data here not reported) shows a strong exothermic decomposition of the Ba phase precursor that is more intense upon increasing the Ba loading. To avoid excessive exothermic phenomena, the samples with the highest Ba content (i.e. the Pt–Ba(23) and Pt–Ba(30) samples) have been calcined according to a slower heating schedule.

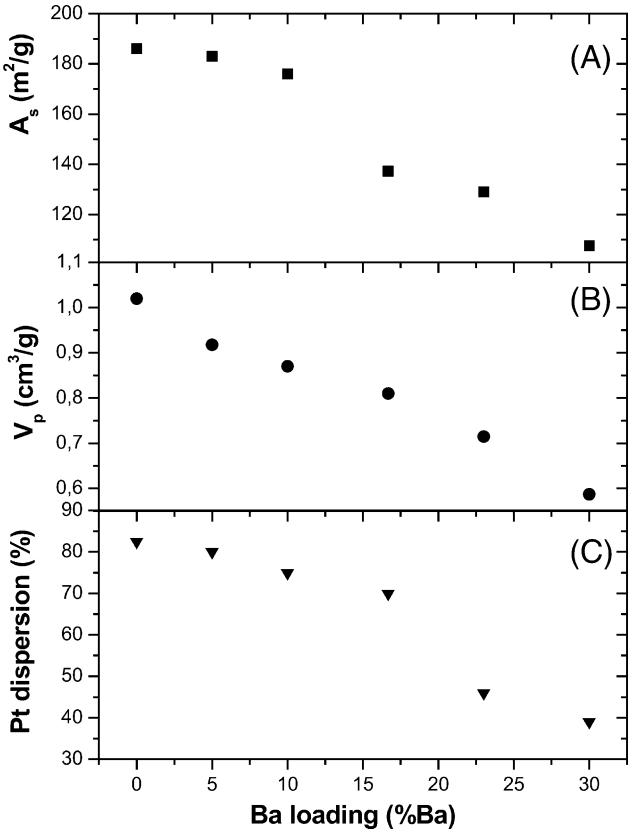

Fig. 1. Morphological properties of the catalysts with different Ba loading: (A) surface area (m^2/g); (B) pore volume (cm^3/g); (C) platinum dispersion (%).

XRD measurements were also performed on the calcined systems for the analysis of crystalline phases. The analysis performed over the investigated Pt–Ba(*x*)/γ-Al_2O_3 samples (Fig. 2) showed in all cases the presence of microcrystalline γ-Al_2O_3 (JCPDS 10-425). In the case of the samples with the lowest Ba content (Pt–Ba(5) and Pt–Ba(10)), no other crystalline phases have been detected, thus suggesting that the Ba component is well dispersed on the support or present as amorphous phase. On the other hand, on the samples with high Ba loading, the presence of crystalline $BaCO_3$ phases (in the monoclinic and orthorhombic, JCPDS 78-2057 and JCPDS5-378, respectively) is evident.

3.2. NO_x storage-reduction

3.2.1. NO_x adsorption process

The results obtained in the case of a rectangular step feed of NO in the presence of 3% (v/v) of oxygen at 350 °C are shown in Fig. 3 for the Pt–Ba(*x*)/γ-Al_2O_3 catalysts. The outlet NO, NO_2 and NO_x ($NO + NO_2$) concentration curves are displayed as a function of time, along with that of the NO inlet concentration (dotted lines).

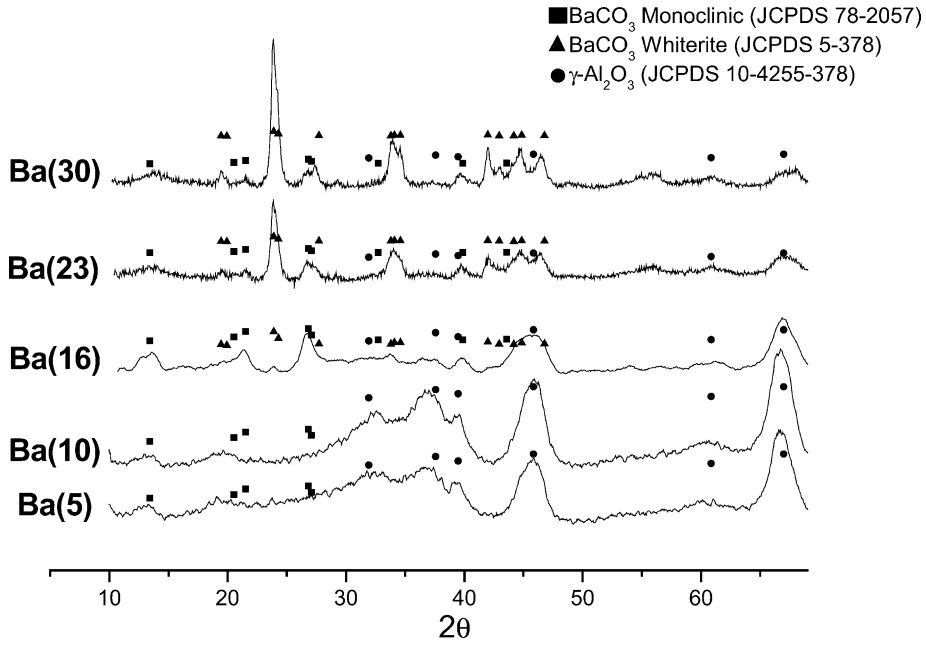

Fig. 2. XRD spectra recorded over Pt–Ba/γ-Al_2O_3 samples with different Ba loadings.

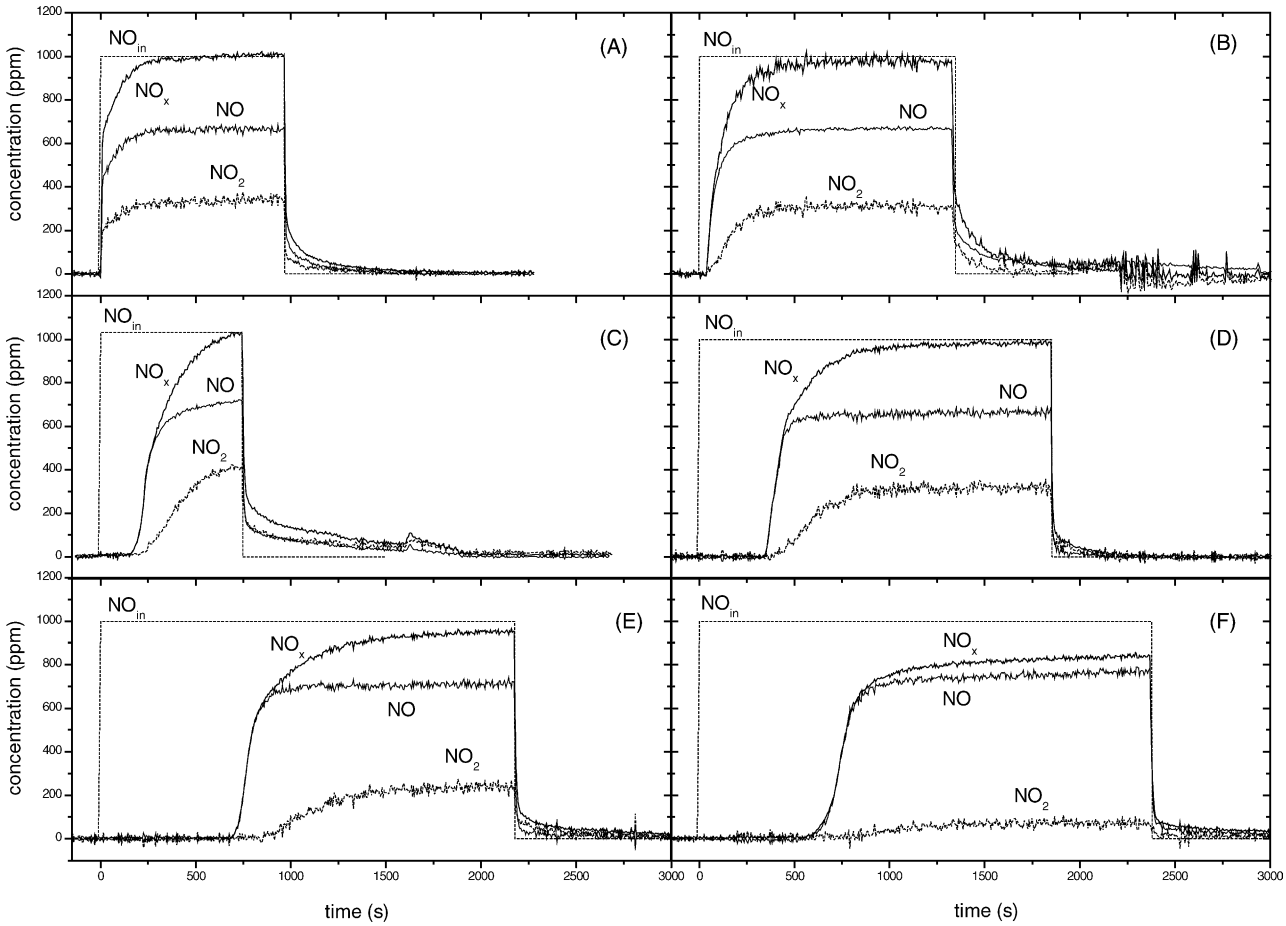

Fig. 3. NO, NO_2 outlet concentration and NO inlet concentration vs. time upon NO addition on the Pt–Ba(*x*)/γ-Al_2O_3 catalysts at 350 °C: (A) Ba(0); (B) Ba(5); (C) Ba(10); (D) Ba(16); (E) Ba(23) and (F) Ba(30) catalysts.

In all cases NO and NO_2 are detected at the reactor outlet, NO_2 formation being ascribed to the occurrence of the oxidation of NO by O_2 according to the stoichiometry of reaction (1):

$$NO + \tfrac{1}{2}O \leftrightarrow NO_2 \quad (1)$$

Taking as reference the Pt–Ba(16) sample (Fig. 3D), the NO outlet concentration shows a dead time of 350 s and then increases with time, up to a steady-state value of about 650 ppm. The NO_2 concentration shows a slightly higher breakthrough time with respect to NO and a much slower approach to its steady-state value, close to 350 ppm. Upon NO shutoff a tail is observed in the NO and of NO_2 concentrations due to the desorption of weakly adsorbed NO_x species, whose release is favored by the decrease in the NO_x partial pressure.

The dead time observed in the NO_x concentration profile (obtained by addition of the NO and NO_2 concentrations) indicates that during the initial part of the pulse the NO fed to the reactor is completely stored on the catalyst surface. As a matter of fact, significant amounts of NO_x are stored during the NO step, as indicated by the area between the inlet and the outlet NO_x concentration traces. In the case of Pt–Ba(16) sample, 4.4×10^{-4} and 6.3×10^{-4} mol NO_x/g_{cat} have been stored at NO_x breakthrough and saturation, respectively.

Notably, from Fig. 3 it appears that the dead time in the NO_x outlet concentration and the NO_2 formation markedly depends on the Ba loading of the catalysts. Concerning the NO_x breakthrough, when NO/O_2 adsorption is carried out on the Pt–Ba(0) sample, no dead time is observed, indicating a negligible storage of NO_x species on the surface. As a matter of facts, only minor amounts of NO_x have been stored in this case up to catalyst saturation, which however desorbs upon closing the NO feed flow. The presence of Ba modifies the response of the catalysts in the adsorption of NO/O_2. In all the cases, the NO outlet concentration shows a dead time that increases from about 180 s for the Pt–Ba(5) sample up to about 600 s for the Pt–Ba(23) and then decreases to 560 s for the sample with the highest Ba content (i.e. 30 wt.%). Also, the tail which is observed upon the NO shutoff in the NO and of NO_2 concentrations (due to the release of weakly adsorbed species) is affected by the catalyst Ba content. At low Ba loading significant amounts of weakly adsorbed NO_x species are released from the catalyst surface, whereas at higher Ba contents lower amounts of NO and NO_2 are observed in the gas phase upon the NO shutoff. This behavior can be associated to the release of NO_x species weakly adsorbed on the alumina surface, whose amount decreases on increasing the catalyst Ba loading due to the higher Ba coverage of the alumina surface. As a matter of facts, it has been shown in previous papers that the thermal stability of adsorbed NO_x species (nitrates and/or nitrites) is higher on Ba with respect to alumina [8,11].

The amounts of NO_x adsorbed on the investigated catalysts up to dead time (NO_x breakthrough) are shown in Fig. 4A. In line with data shown in Fig. 3, a more than linear increase in the amounts of stored NO_x is observed upon increasing the Ba content of the catalyst up to 8×10^{-4} mol NO_x/g_{cat} for the Pt–Ba(23) system. These data agree with some literature indications [3,18].

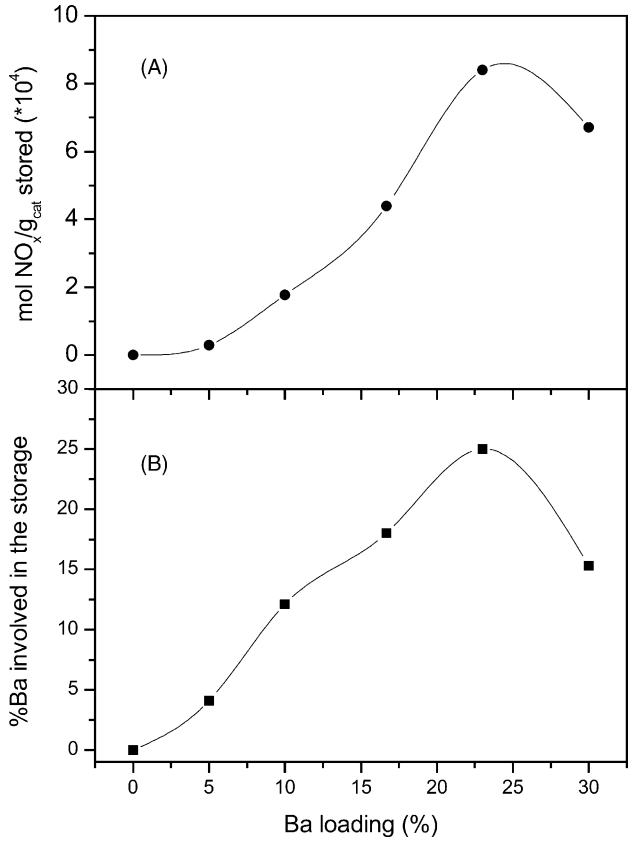

Fig. 4. (A) Moles of NO_x adsorbed (mol/g_{cat}) and (B) fraction of active Ba vs. Ba loading up to NO_x breakthrough on Pt–Ba(x)/γ-Al_2O_3 catalysts.

It is of interest to evaluate for the various samples the fraction of Ba that participates in the storage process ("active" Ba), i.e. the % ratio of Ba involved in the storage with respect to the total amount of Ba present in the catalyst sample. Considering the formation of either $Ba(NO_2)_2$ or $Ba(NO_3)_2$ the amounts of Ba participating in the process can be calculated from the amounts of NO_x species adsorbed during the storage periods. The amounts of "active" Ba are shown in Fig. 4B as a function of the Ba loading. It appears that the fraction of Ba involved up to NO_x breakthrough is low (about 4%) for Pt–Ba(5) sample, and then increases linearly with the catalyst Ba content and up to the maximum value of about 25% for the Pt–Ba(23) sample, which accordingly exhibits the best exploitation of the Ba component. Notably, the estimation of the Ba coverage for the different samples showed that a value close to 1 was almost achieved for Ba content of 16–20% (w/w): this suggests that the maximum storage capacity is presented by the systems which are characterized by the formation of the monolayer.

These results appear at a variance of the data obtained by Laurent et al. [18], who reported that less than 1% of barium is involved in the storage since a large amount of

BaO is unavailable for the adsorption process. The authors conclude in this case that only the grains that are in close contact with platinum sites are those reactive in the process.

From data reported in Fig. 3, it clearly appears that for all the investigated catalysts NO_2 was detected at the reactor outlet, due to NO oxidation according to reaction (1). In all cases the evolution of NO_2 shows a larger delay with respect to that observed for the NO concentration; then, the NO_2 concentration slowly increases with time, reaching a constant value at catalyst saturation. Also, upon increasing the Ba loading, a slower NO_2 response to its steady state is observed, so that at the highest investigated Ba content the catalyst is apparently not yet saturated with NO_x after 2000 s.

At the end of the pulse, similar NO and NO_2 concentrations (600 and 300 ppm, respectively) have been observed in the case of the samples with Ba loading lower than 16% (w/w), thus suggesting that the presence of barium does not significantly modify the oxidant capacity of the catalytic systems. As a matter of facts, since both the Pt weight % and its dispersion decrease on increasing the Ba content (from 0.99 to 0.83% and from 85 to 38%, respectively; see Table 1 and Fig. 1C), it might be speculated that the reactivity of Pt sites towards NO oxidation is increased. This clearly appears from the analysis of Fig. 5, where the NO_2/NO ratio estimated at catalyst saturation is plotted as a function of the Ba loading (Fig. 5A) and of the "active Pt content" of the samples (i.e., the Pt catalyst weight % estimated by Pt dispersion, Fig. 5B). The corresponding value of chemical equilibrium is also reported (dashed line). Up to 16% of Ba content, which correspond to the higher value of active Pt, the NO_2/NO calculated ratio does not vary significantly and it remains of the same order of magnitude of the thermodynamic equilibrium value. The fact that the outlet concentration of NO_2 is not apparently affected by the decreased active Pt content of the catalysts, suggest an increased activity of Pt sites upon Ba addition that could be related to an electronic interaction between Pt and Ba. As a matter of facts, the existence of a strong Pt–Ba interaction has already been evidenced in previous works [11,22].

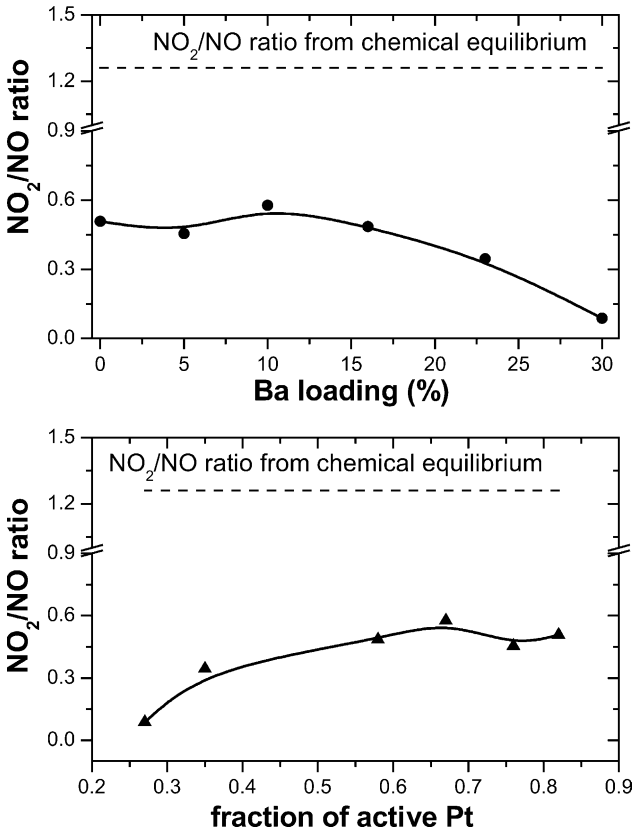

Fig. 5. NO_2/NO ratio at catalyst saturation and the corresponding value of chemical equilibrium at 350 °C.

However, on the samples with the highest Ba contents (23 and 30%) a decrease in the NO_2 outlet concentration (from 100 to 350 ppm) at catalyst saturation is observed, accompanied by a correspondent increase of the NO outlet concentration (from 650 to 800 ppm). This seems to indicate that at high Ba content the oxidant capacity of the catalytic system is apparently decreased. This is also evident from Fig. 5, where marked deviations in the NO_2/NO ratio from those corresponding to chemical equilibrium were observed on increasing the Ba content. However, this behavior is associated with a lower content of the active Pt in the catalysts, so that the decrease in the oxidant capability of the systems may be uniquely related to the decrease of the Pt content (also due to Ba masking), and not to a decrease of the Pt activity. These aspects are currently object of further studies in our laboratories.

Inspection of Fig. 4A and B clearly points out that the NO_x storage capacity, which increases with the Ba loading, seems to be independent from the oxidative capability of the catalysts. As a matter of fact, the samples which exhibit the highest NO_x adsorption capability (i.e. Pt–Ba(23) and Pt–Ba(30)) also showed the lowest efficiency in the oxidation, i.e. lowest formation of NO_2. This apparently contrasts with the most common NO_x adsorption mechanism reported in the literature that consider as first adsorption step the oxidation of NO to NO_2 followed by the adsorption of NO_2 in the form of nitrates. In line with this mechanism, it is expected that this pathway requires a good oxidant capability of the catalyst, which however is apparently not present on the samples with the highest Ba loading. On the other hand, we have proposed in previous papers a different NO_x storage pathway (the "nitrite" route), which involves the direct NO uptake in the presence of oxygen on the Ba component to form nitrite ad-species. These nitrite species are then oxidized to nitrates. To better clarify this point, NO adsorption experiments in the presence of oxygen have been performed over a mechanic mixture of Pt/γ-Al_2O_3 and Ba/γ-Al_2O_3 having the same Pt and Ba loading of the Pt–Ba(16) sample. The data recorded (here not reported) showed that the mechanical mixture confirm the storage mechanism proposed in literature where NO is oxidized to NO_2 at first; NO_2 is adsorbed on the catalytic surface to form nitrates. In this case, no direct interaction is necessary to have a good and efficient adsorption.

Accordingly to the mechanism proposed by us [11], gaseous O_2 is activated by Pt sites, and transferred to neighbor Ba sites. This would favor a stepwise oxidative adsorption of NO in the form of nitrite-like ad-species on the Ba sites. Accordingly, a cooperative effect between Pt–Ba neighboring couples appears to be relevant for this route. Hence, it can be speculated that the higher the number of Pt–Ba neighboring couples, the higher the efficiency of the "nitrite" route and of the NO_x storage.

As a matter of fact, the characterization analysis reported above clearly indicated that Pt is well dispersed on the catalyst surface before Ba addition. Upon impregnation with the Ba precursors, barium surface species may remain statistically close to Pt. Accordingly, it may be speculated that on increasing the Ba loading the possibility to have Pt–Ba neighboring species is also increased. Neighbors Pt–Ba species would favor the NO_x storage process according to the "nitrite" pathway, thus resulting in a better utilization of the Ba component.

Of course, when the Ba content is excessively increased, Pt sites might be covered by the Ba phase. Accordingly, the Pt dispersion is decreased (as indeed observed) and the Pt–Ba interaction is no further enhanced, as likely occurring in the Pt–Ba(30) sample. This hypothesis is in line with the suggestion of Fanson et al. [20] who performed FT-IR spectra after CO adsorption at room temperature on Pt–Ba(8)/γ-Al_2O_3 and on Pt–Ba(26)/γ-Al_2O_3. The authors showed that the interaction between the platinum and the barium is much greater for the catalyst with the higher Ba content and that the majority of the platinum sites on Pt–Ba(8)/γ-Al_2O_3 are isolated from the BaO phase. They concluded that a high Ba loading (c.a. 25 wt.%) is necessary to ensure proper contact with the Pt particles and hence necessary for a significant adsorption of NO.

The fact that the presence of Pt–Ba neighboring couples could play a positive effect on the storage capacity of the catalyst was also addressed and proposed by some of us in [11], and in agreement with the picture presented by Mahzoul et al. [3]. Indeed, their data indicate that when more BaO crystallites are present and accessible to NO, more Pt sites located close to Ba are available and more ads-species formation occurs. So, a good dispersion of barium would increase the storage capacity. On the other hand, Pt sites, which are located too far from BaO crystallite to allow the adsorption of NO, promote instead the NO oxidation to NO_2 that is released in the gas phase.

3.2.2. NO_x reduction

The reduction of the stored NO_x (i.e. catalyst regeneration) has been carried out with H_2 (2000 ppm) in He. The results are showed in Fig. 6, in terms of H_2, N_2, NH_3 and H_2O outlet concentration curves and H_2 inlet concentration with time for all the Pt–Ba(x) catalysts.

As discussed above, the Pt–Ba(0) catalyst showed no significant storage capacity of NO under lean condition and accordingly no N_2 is formed upon the H_2 switch over this sample. As a matter of facts, FT-IR data reported in a previous work [11] have demonstrated that very small amounts of surface nitrites were formed at low contact times (up to 5 min) and that they were then slowly oxidized to nitrate species. In any case, at the end of the desorption process no significant amounts of adsorbed species are present on the catalyst surface as confirmed by the reducing procedure (Fig. 6A), which did not show any consumption of hydrogen or formation of nitrogen.

A different picture is apparent for the Pt–Ba(5) catalyst: indeed, in this case NO_x adsorbed species are stored on the catalytic surface after the NO_x adsorption phase, so that upon H_2 step addition to the reactor the reduction reaction takes place. From the analysis of the concentration curves reported in Fig. 6B, it clearly appears that upon H_2 admission ($t = 0$ s) the NO_x adsorbed species are readily reduced as indicated by the complete H_2 consumption and the correspondent evolution of N_2 and H_2O (this last species not reported in the Figure). The reduction process is very fast and after 115 s it is completed; then the H_2 concentration increases with time, reaching the inlet value (2000 ppm).

The adsorbed nitrate species are reduced to nitrogen according to the following reaction:

$$2NO_3^- + 5H_2 \rightarrow N_2 + 5H_2O + O^{2-} \quad (2)$$

Data reported in Fig. 6 indicate the almost stoichiometric occurrence of reaction (2) (the N-balance closed within 5%), while very small amounts of NO (not shown in the figure) were formed during the catalyst regeneration. Accordingly the reduction process appears to be very selective towards the formation of nitrogen.

When the Ba loading increases up to 10% w/w (Fig. 6C), the reduction step is longer than in the previous case, in line with the higher amounts of NO_x species stored during the previous adsorption phase; indeed, the quantity of N_2 formed following reaction (2) is proportional to the quantity of stored NO_x. Also in this case, very low amounts of NO were found at the reactor outlet so that the reduction process is still very selective.

A different picture was observed for the Pt–Ba(x) samples with higher Ba content (Fig. 6D and F). In line with the major amounts of NO_x stored at higher Ba content, the reduction step requires a longer time to be completed. Furthermore, during the reduction process, the formation of NH_3 is also observed, whose amounts increases on increasing the Ba loading of the catalyst. Notably, the reduction process is initially selective to N_2; once the N_2 production is terminated, ammonia appears at the reactor outlet.

On the basis of the data above presented it results that for Ba loading higher than 16%, the reduction process should consider the occurrence of reaction (2), which leads to N_2, but also of the following reaction:

$$2NO_3^- + 8H_2 \rightarrow 2NH_3 + 5H_2O + O^{2-} \quad (3)$$

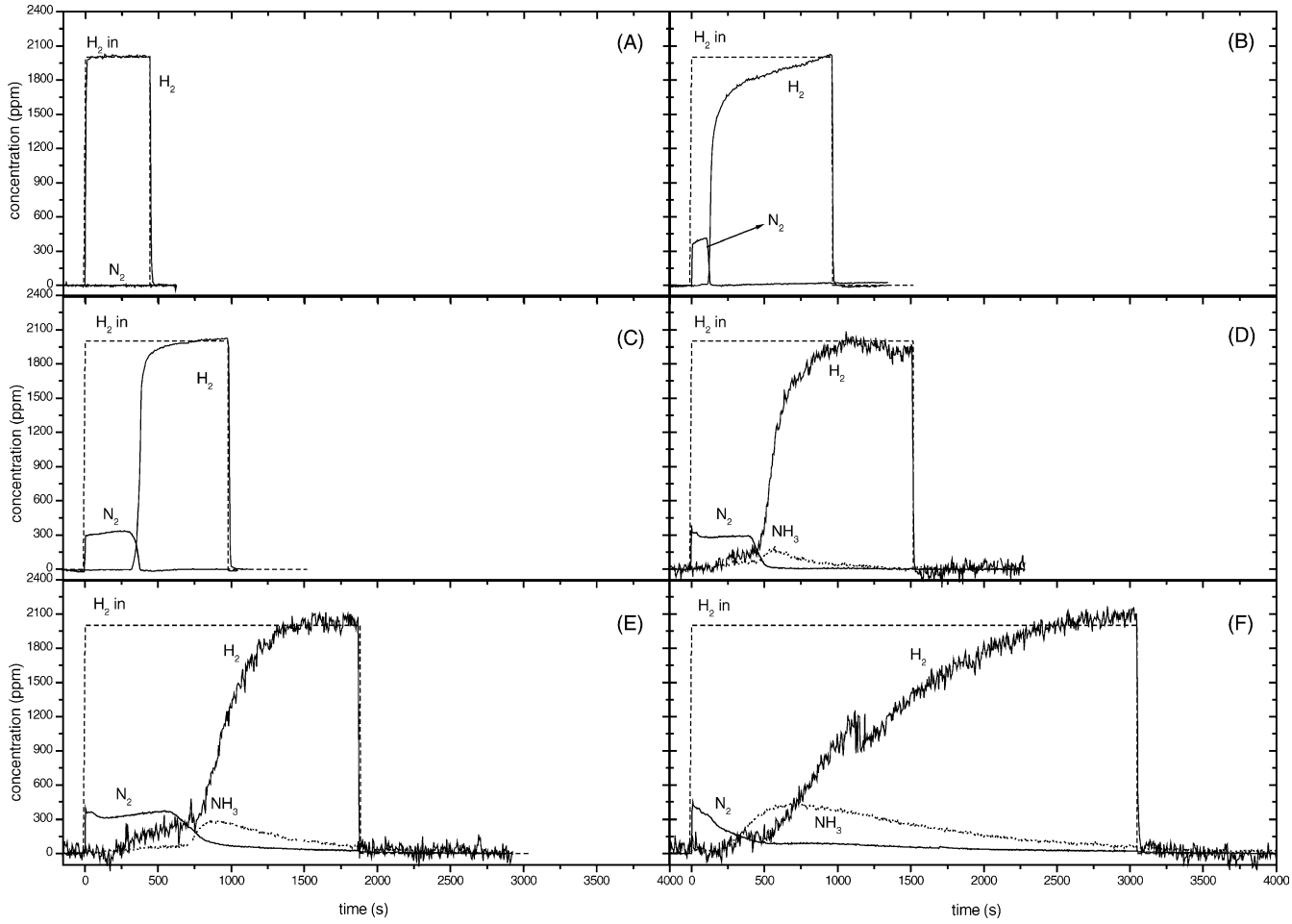

Fig. 6. N_2, NH_3, H_2O, H_2 outlet concentrations and H_2 inlet concentration vs. time upon H_2 addition on the Pt–Ba(x)/γ-Al_2O_3 at 350 °C: (A) Ba(0); (B) Ba(5); (C) Ba(10); (D) Ba(16); (E) Ba(23) and (F) Ba(30) catalysts.

which accounts for NH_3 production. As a matter of facts, N_2 selectivity values as low as 30% have been measured for the Pt–Ba(30) sample (see below, Fig. 7).

It is worth noticing that the concentration profiles of nitrogen and ammonia suggest a consecutive reaction scheme of the two reduction processes, although different hypothesis cannot be ruled out. As previously observed, N_2 is immediately observed upon H_2 admission and its concentration is constant for a certain period. Accordingly, reaction (2) is very fast and limited by the hydrogen concentration. Then, when nitrogen concentration decreases, the slower reaction (3) takes place, giving NH_3. As a matter of fact, the higher the amounts of produced NH_3, the slower the increase of the H_2 concentration profile. Notably, the ratio "H_2 consumed/NH_3 produced" (evaluated from the experimental H_2 and NH_3 curves and taking into account the amounts of H_2 consumed in the reduction of adsorbed nitrates to N_2 according to the stoichiometry of reaction (2)) approaches the stoichiometric value of 4 from reaction (3), which is hence representative of the reduction process.

The data reported in Fig. 7 show the behavior of the selectivity (calculated as: $[2\,N_2]/([NO] + [2\,N_2] + [NH_3])$) measured during the reduction of the adsorbed NO_x species (reduction phase) and the NO_x dead time measured during the NO_x adsorption (storage phase) as a function of the Ba content. It clearly appears that the catalyst samples which show the highest storage capability are on the other hand characterized by low selectivity during the reduction phase. Notably, the decrease in selectivity is associated with Ba coverage approaching the monolayer formation.

The match of data above presented and discussed evidenced that the reduction process is complex and that it can lead to nitrogen and/or ammonia depending on the formulation and properties of the catalysts. A comprehensive and detailed picture explaining the mechanism of the reduction process and in particular of its selectivity have not been yet proposed in the literature, and it is currently under investigation in our laboratories. However, it clearly appears that the reduction process seems to be catalyzed by Pt particles, which play a very important role in the decomposition of surface nitrate species. As suggested by Fanson et al. [20], the primary role of platinum should be allowing the reducing agent to bond the surface, which can then react with stored nitrates.

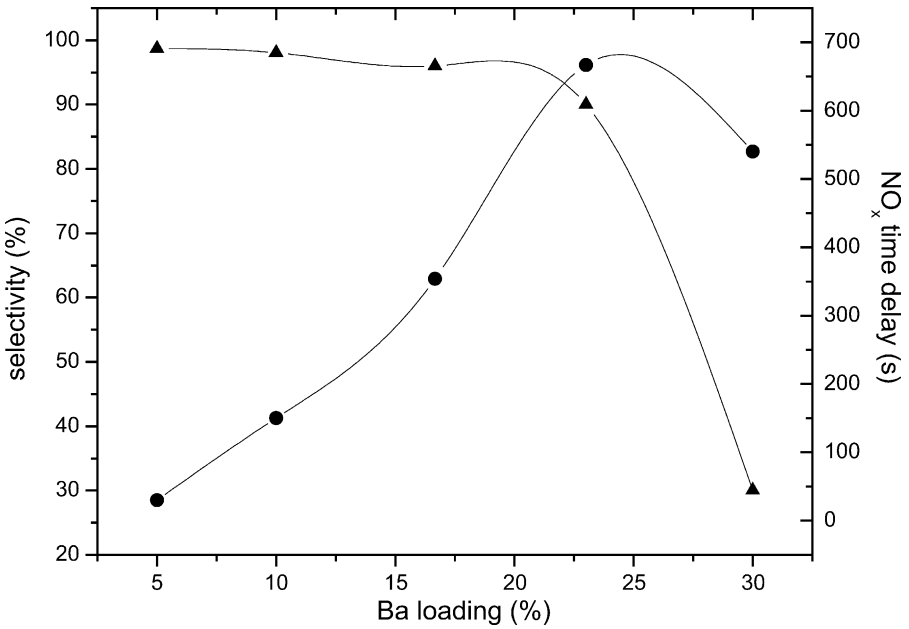

Fig. 7. Selectivity behavior during reduction of the adsorbed NO_x species (reduction phase) and NO_x dead time upon NO_x adsorption (NO_x storage) vs. Ba loading.

James et al. [23] studied a $Pt/Ba(NO_3)_2/Al_2O_3$ powdered system with a pulse-flow reactor connected with a mass spectrometer. From their experiments, the authors proposed that on moving towards rich conditions, some of the nitrate ad-species could be released and decomposed to NO, which is then reduced by the Pt alone. It should be noted that if the mechanism proposed by these authors is operating, the selectivity in the reduction process should be related to Pt itself or to the Pt–Ba interaction, which in line with our results is apparently an important issue in these catalysts. In addition, it is worthy of note that very small amounts, if any, of NO were detected during the reduction periods.

A different picture is suggested by Daturi and coworkers [24]; they used in situ FT-IR spectroscopy coupled with mass spectroscopy to study the mechanism of NO_x storage and reduction over a $Pt–Rh/Ba/Al_2O_3$ NO_x storage catalyst. In line with the James hypothesis, the authors proposed that the effect of the reducing agent is to decompose the adsorbed species into NO, which is subsequently dissociated by the reduced metal. They also observed that the reduction process is not completely selective towards nitrogen, since significant amounts of ammonia were detected; the formation of this species was ascribed to direct reaction of hydrogen with NO or to hydrolysis of isocyanates (formed simultaneously with nitrates during the storage phase), following the stoichiometry:

$$2NCO + 3H_2O \rightarrow 2NH_3 + 2CO_2 + \tfrac{1}{2}O_2 \quad (4)$$

This picture explains the formation of nitrogen and ammonia during the reduction according to the presence of different adsorbed species, i.e. nitrates and isocyanates. This datum could be in agreement with our experimental observations, but the proposed mechanism requires the presence of isocyanates species and thus of carbonates on the catalyst surface and this in contrast with our results that showed that after conditioning of the catalysts the active phase for the NO_x storage is BaO; in any case, further experiments are necessary to characterize the surface species formed on catalysts with different Ba loadings.

In conclusion the formulation of a mechanism for the reduction of NO_x species over $Pt–Ba/Al_2O_3$ samples should account for the experimental evidences collected and above presented, such as: (i) the absence of significant amounts of NO formation during the reduction, which some authors proposed as intermediate species in the nitrogen formation; (ii) the formation of ammonia, which has been possibly related to the existence of isocyanates species; (iii) the decrease in the selectivity on increasing the Ba loading of the catalysts, associated with an increased production of ammonia.

4. Conclusions

In this paper, we have investigated the effect of Ba loading 0–30% (w/w) in the storage and reduction over $Pt–Ba/Al_2O_3$ samples.

The results indicated that the addition of Ba affected negatively both the morphological properties and the noble metal dispersion for the systems with Ba loading higher than 10%.

Nevertheless, the increase in the Ba loading resulted in a strong increase of the NO_x adsorption at breakthrough, as showed by the NO/O_2 experiments carried out at 350 °C. Under these conditions, a maximum value of adsorbed NO_x species close to 8×10^{-4} moles/g catalyst was observed for the $Pt–Ba(23)/Al_2O_3$ sample. Simultaneously, the addition of Ba resulted in an increase of the percentages of Ba

involved in the storage: a maximum value of ca. 25% was evaluated for the system with 23% (w/w) of Ba content.

The increase of the catalyst capability to adsorb NO with the Ba loading has been associated to the involvement in the NO_x storage process of Pt–Ba neighboring species: in facts, the addition of Ba increases the number of Pt–Ba neighboring species, which could favor the NO_x storage process, resulting in a better utilization of the Ba component.

The analysis of the storage phase showed also that the higher Ba content the lower was the NO_2 concentration value at catalyst saturation, this effect being marked for the highest Ba loadings: this effect is related to the decrease in the Pt content associated with the Ba addition to the samples and to a possible masking of Pt sites when the Ba coverage approaches and exceeds the monolayer formation. The fact that the NO_x storage capacity seems to be independent from the oxidative capability of the catalysts is apparently in contrast with the NO_x adsorption mechanism reported in the literature, which consider the oxidation of NO to NO_2 as the first necessary step for the storage of NO_x species.

For all the investigated catalysts, the stored NO_x species are readily reduced upon H_2 admission as indicated by the complete H_2 consumption and the correspondent evolution of N_2 and H_2O. When the Ba content of the samples was higher than 16%, at the end of the N_2 production ammonia appears at the reactor outlet: accordingly these catalysts were characterized by a lower selectivity, which were close to 30% for the Pt–Ba(30) sample.

The match of data collected evidenced that the reduction process is very complex and that it can lead to nitrogen and/or ammonia depending on the formulation and properties of the catalysts. A comprehensive and detailed picture explaining the mechanism of the reduction process and in particular of its selectivity is currently under investigation in our laboratories.

References

[1] H. Shinjoh, N. Takahashi, K. Yokota, M. Sugiura, Appl. Catal. B 15 (1998) 189.
[2] E. Fridell, M. Skoglundh, B. Westerberg, S. Johanson, G. Smedler, J. Catal. 183 (1999) 196.
[3] H. Mahzoul, J.F. Brilhac, P. Gilot, Appl. Catal. B 20 (1999) 47.
[4] I. Nova, L. Castoldi, L. Lietti, E. Tronconi, P. Forzatti, Catal. Today 75 (2002) 431.
[5] N.W. Cant, M.J. Patterson, Catal. Today 73 (2002) 271.
[6] L. Lietti, P. Forzatti, I. Nova, E. Tronconi, J. Catal. 204 (2001) 175.
[7] E. Fridell, M. Skoglundh, B. Westerberg, S. Johansson, G. Smedler, J. Catal. 183 (1999) 196.
[8] F. Prinetto, G. Ghiotti, I. Nova, L. Lietti, E. Tronconi, P. Forzatti, J. Phys. Chem. B 105 (2001) 12732.
[9] E. Fridell, H. Persson, B. Westerberg, L. Olsson, M. Skoglundh, Catal. Lett. 66 (2000) 71.
[10] B. Westerberg, E. Fridell, J. Mol. Catal. A: Chem. 165 (2001) 249.
[11] I. Nova, L. Castoldi, L. Lietti, F. Prinetto, G. Ghiotti, E. Tronconi, P. Forzatti, J. Catal. 222 (2) (2004) 377.
[12] J.A. Anderson, B. Bachiller-Baeza, M. Fernández-García, Phys. Chem. Chem. Phys. 5 (2003) 4418.
[13] C. Hess, J.H. Lunsford, J. Phys. Chem. B 106 (2002) 6358.
[14] L. Olsson, B. Westerberg, H. Persson, E. Fridell, M. Skoglundh, B. Andresson, J. Phys. Chem. B 103 (1999) 10433.
[15] L. Olsson, H. Persson, E. Fridell, M. Skoglundh, B. Andresson, J. Phys. Chem. B 105 (2001) 6895.
[16] L. Olsson, E. Fridell, M. Skoglundh, B. Andresson, Catal. Today 73 (2002) 263.
[17] A. Scotti, I. Nova, E. Tronconi, L. Castoldi, L. Lietti, P. Forzatti, Kinetic Study of Lean NO_x Storage over Pt–Ba/Al_2O_3 System, IEC Research, in press.
[18] F. Laurent, C.J. Pope, H. Mahzoul, L. Delfosse, P. Gilot, Chem. Eng. Sci. 58 (2003) 1793.
[19] I. Nova, L. Castoldi, F. Prinetto, V. Dal Santo, L. Lietti, E. Tronconi, P. Forzatti, G. Ghiotti, R. Psaro, S. Recchia, Topics Catal. 30/31 (2004) 181.
[20] P.T. Fanson, M.R. Horton, W.N. Delgass, J. Lauterbach, Appl. Catal. B 46 (2003) 393.
[21] C. Hess, J.H. Lunsford, J. Phys. Chem. B 107 (2003) 1982.
[22] I.V. Yentekakis, M. Konsolakis, R.M. Lambert, N. Macleod, L. Nalbantian, Appl. Catal. B 22 (1999) 123.
[23] D. James, E. Fourré, M. Ishii, M. Bowker, Appl. Catal. B 45 (2003) 147.
[24] T. Lesage, C. Terrier, P. Bazin, J. Saussey, M. Daturi, Phys. Chem. Chem. Phys. 5 (2003) 4435.